


RESEARCH

Open Access



# Comprehensive nontargeted analysis of fluorosurfactant byproducts and reaction products in wastewater from semiconductor manufacturing

Yi-Ju Chen<sup>1,2</sup>, Jheng-Sian Yang<sup>2</sup> and Angela Yu-Chen Lin<sup>2\*</sup> 

## Abstract

Semiconductor manufacturing employs per- and polyfluoroalkyl substances (PFAS) as fluoroasurfactants to enhance the quality of photolithography lines. Our research, employing a fragment-based approach to investigate nontarget PFAS, overcomes conventional homologous series limitations. In a mixture of PFAS standards used as a quality control sample, 92% (36 out of 39 compounds spanning 11 compound classes) were detectable through the fragment-based nontarget procedure. This indicates the effectiveness of this approach in identifying the hydrophobic and hydrophilic characteristics of various fluorosurfactants. Eighty-three PFAS were detected in wastewater and effluent samples from semiconductor industry, including 29 newly discovered compounds, categorized into three groups. First, besides detecting perfluorobutane sulfonamido ethanol (FBSE), various fluoroalkyl chain structures of FBSE derivatives were initially identified in wastewater. These include perfluorobutyl ether sulfonamido ethanol, unsaturated FBSE, and hydrogen-substituted FBSE. These derivatives were also detected in trace amounts in commercial authentic standards of FBSE. To quantify their presence, we analyzed the FBSE derivatives from the authentic standard, and the relative proportions of these derivatives contribute to approximately 0.5%. This suggests that the FBSE derivative series detected in wastewater may arise from byproducts of chemical formulations used in the manufacturing of semiconductors. Second, transformation products from FBSE during oxidation, including the first identified intermediate transformation compounds, perfluorobutane sulfonamido acetaldehyde and its hydrate, were discovered. Third, diverse reaction products are generated from the intricate processes of semiconductor manufacturing, which utilize strong acids, bases, and solvents under UV light or heated conditions. These processes include the formation of PFAS-related compounds through hydration, sulfonation, oxidation, and nitrification. This study revealed 25 isomeric PFAS, encompassing headgroup isomers and functional tail group isomers. These findings underscore the importance of comprehending diverse reactions and the overall emission compositions of PFAS in semiconductor wastewater, highlighting its complexity and presenting challenges for subsequent wastewater treatment.

**Keywords** Per- and polyfluoroalkyl substances, PFAS, Semiconductor, Perfluorobutane sulfonamido ethanol, Perfluorobutane sulfonamide, Transformation products, Byproducts, Aldehyde hydration

\*Correspondence:

Angela Yu-Chen Lin  
yuchenlin@ntu.edu.tw

Full list of author information is available at the end of the article



© The Author(s) 2024. **Open Access** This article is licensed under a Creative Commons Attribution 4.0 International License, which permits use, sharing, adaptation, distribution and reproduction in any medium or format, as long as you give appropriate credit to the original author(s) and the source, provide a link to the Creative Commons licence, and indicate if changes were made. The images or other third party material in this article are included in the article's Creative Commons licence, unless indicated otherwise in a credit line to the material. If material is not included in the article's Creative Commons licence and your intended use is not permitted by statutory regulation or exceeds the permitted use, you will need to obtain permission directly from the copyright holder. To view a copy of this licence, visit <http://creativecommons.org/licenses/by/4.0/>.

## 1 Introduction

Perfluoroalkyl and polyfluoroalkyl substances (PFAS) have been extensively utilized in various industrial processes and commercial products, including food packaging, stain repellents, building materials, electronic devices, and firefighting foams [1, 2]. The Organization for Economic Co-operation and Development expanded the scope of fluorochemicals in its 2021 revision of the PFAS definition, classifying PFAS as fluorinated substances with at least one fully fluorinated methyl ( $-\text{CF}_3-$ ) or methylene ( $-\text{CF}_2-$ ) carbon atom [3, 4]. PFAS, with fluorine-substituted aliphatic carbon backbones, exhibit stability, low refractive index, and hydrophobic/oleophobic properties [5], making them valuable for industrial surfactants [6]. Perfluorooctane sulfonate (PFOS), once dominant in semiconductor manufacturing processes in etching silica [7] and serving as a photoacid generator [8], was detected at high concentrations in photolithographic wastewater ( $12.6 \text{ mg L}^{-1}$ ) and semiconductor effluents (up to  $0.13 \text{ mg L}^{-1}$ ) [9]. Following the phased replacement of PFOS in the semiconductor industry, short chain as perfluorobutane sulfonate (PFBS) emerged as a predominant compound, ranging from  $0.127$  to  $8.04 \mu\text{g L}^{-1}$  in wastewater [10, 11]. Additionally, ultrashort perfluoroalkyl acids such as trifluoroacetic acid (TFA) and perfluoropropionic acid (PFPrA) were reported in wastewater, with concentrations ranging from  $0.004$  to  $19.9 \mu\text{g L}^{-1}$  [10, 12]. Our previous study emphasized the prevalence of neutral C4 sulfonamido derivatives, such as perfluorobutane sulfonamido ethanol (FBSE), perfluoro-sulfonamide (FBSA), and perfluorobutane sulfonamido diethanol (FBSEE diol) as emerging fluorosurfactants, reaching maximum concentrations of 482, 141, and  $83.5 \mu\text{g L}^{-1}$  in wastewater [10]. Previous discoveries have primarily focused on perfluoroalkyl substances, fewer reports focused on variation on fluoroalkyl chains and transformation products involving different headgroups of PFAS.

PFAS have aroused concern owing to their health [13] and environmental impact [14]. Under the Toxic Substances Control Act Sect. 8(a)(7), the United States Environmental Protection Agency mandates reporting regulations for PFAS in 2023, requiring manufacturers and processors to submit detailed information on PFAS substance usage from 2011 to 2022, covering identification, applications, quantities, environmental impacts, and health effects [15]. Perfluorohexanesulfonic acid (PFHxS) including its salts and over one hundred PFHxS-related compounds, defined as structures containing  $\text{C}_6\text{F}_{13}$  capable of degrading into PFHxS [16], have been listed in the Stockholm Convention to restrict and eliminate their use since 2022. A significant portion of PFHxS-related compounds primarily comprises sulfonamides and

sulfonamido substances, posing challenges in analysis due to the lack of authentic standards. Despite the convention's recommendation to use total oxidizable precursors [17] and extractable organic fluorine [18] to assess the presence of precursors, methods for identifying individual compounds are currently unavailable [19].

To identify nontarget PFAS, high-resolution tandem mass spectrometry has been used widely in contaminated soil [20], surface water [21], wastewater from a fluorochemical manufacturing [22], and municipal wastewater [23]. Mass defect and homologous patterns are potent tools for uncovering PFAS within a series of homologous substances. Chemicals utilized in industrial processes display diverse and precise functionalizations, and the complex blend in wastewater prompt various reactions like hydration, oxidation, and deamination [24, 25]. Given that these reactions occur mostly in the polar functional section, each transformation yields distinct mass defect values, making the utilization of homologous patterns for screening impractical. Consequently, our research employed a fragment-based approach to investigate PFAS-related substances by screening the polar functional groups and nonpolar fluoroalkyl chains of fluorosurfactants. Ten wastewater samples from five semiconductor plants and three effluents from their associated wastewater treatment plants (WWTPs) were investigated for comprehensive identifications of PFAS-related byproducts of chemical formulations, transformation products generated during the oxidation process, and diverse reaction products generated from the intricate processes of semiconductor manufacturing.

## 2 Materials and methods

### 2.1 Sampling

In November 2020 and January 2021, ten wastewater samples (no. 184–187, 190, 191, 194–197) were collected from five semiconductor plants (A, B, C, D, E) situated in three different Science Parks, along with three effluent samples (WWTP I, WWTP II, WWTP III) from their respective wastewater treatment plants, as depicted in Fig. S1 of Supplementary Materials (SM). We collected wastewater downstream from each factory, prior to its entry into the main wastewater pipe. Hence, the wastewater is specifically attributed to the discharge of each factory. In addition, effluents were gathered from discharge points of wastewater treatment plants, all employing the activated sludge process. The samples were kept in 1 L polypropylene bottles and sent to the laboratory at  $4 \text{ }^\circ\text{C}$  for analysis.

### 2.2 Pretreatment

A solid phase extraction cartridge (Oasis WAX, Waters) features a weak anion-exchange and reversed-phased

sorbent was applied to condense water samples. The capture strategy involves performing the load and wash procedures at  $\text{pH} < 3$ . The elution is performed at a neutral  $\text{pH}$  for neutral PFAS and at a  $\text{pH} > 8$  for acidic PFAS. Detailed pretreatment procedures are included in the SM.

### 2.3 Analysis

Table S1 in SM lists authentic reference standards used to establish the patterns for scanning fragmentation and neutral loss values in PFAS screening. Table S2 includes lists of authentic reference standards employed to confirm the identified PFAS. The injection of a 50–100  $\mu\text{L}$  extract was carried out using a UPLC binary pump system and interfaced with a negative electrospray ionization source coupled to a Q-Exactive hybrid mass spectrometer. The mass spectrometric analysis was conducted in full MS and 20 data-dependent MS2 scans, involving a full scan analysis ranging from  $m/z$  77–1155 with applied fragmentation energy (NCE 15 and 50). Mass calibration

before each analysis ensured accurate results, and the inclusion of acetic acid in the calibration solution is crucial to enhance mass accuracy, especially for low mass measurements. Specific details regarding the LC gradient program and mass spectrometry settings can be found in Table S3.

The data analysis workflows for nontarget analysis of PFAS are illustrated in Fig. 1. Thermo Scientific Compound Discoverer 3.3 software was employed for compound detection and identification (Fig. S2). In particular, the Compound Class Scoring node (MS2) and the Search Neutral Losses node (MS2) were utilized for searching fragments and neutral losses, respectively, while the Search for ChemSpider node screened databases based on formulas within a 5 ppm mass tolerance (MS1). The detailed specifications of the workflow nodes are outlined in Table S4. The identification confidence levels (CLs) were adapted from Charbonnet's classification [26], as illustrated in Table S5. In databases equipped with an MS2 library (e.g. mz cloud), the matching is classified as

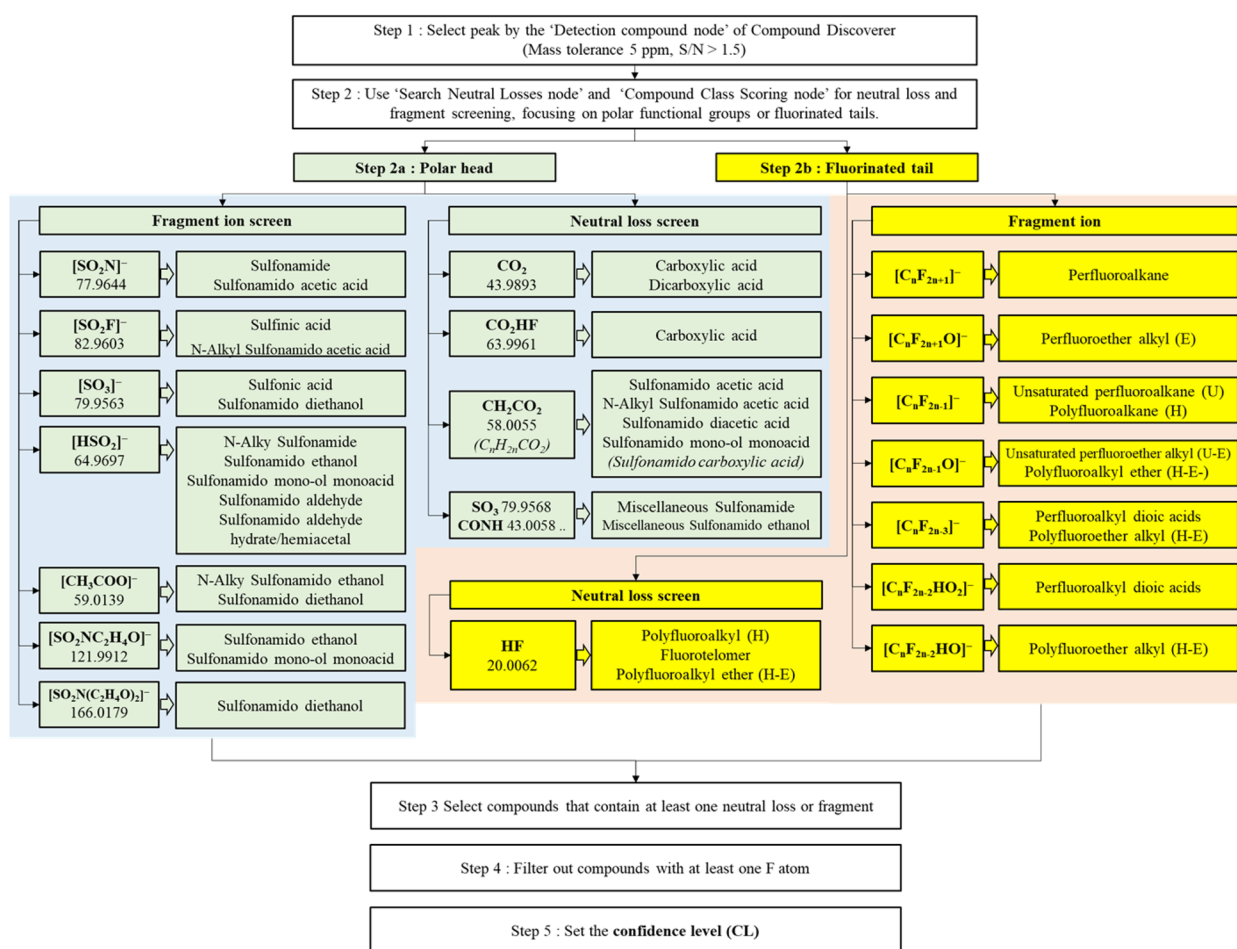


**Fig. 1** The workflow of nontarget analysis

CL2a. In databases that provide only formula information without MS2 libraries, identification relying on formula matching (isotope pattern matching, MS1) is classified as CL4. Moreover, CL is determined by the quantity of fragments, with a single fragment corresponding to CL3, while two or more fragments are classified as CL2 or above. Based on the scope of identification, we divided our analysis into two aspects: CL1-identified PFAS and tentatively identified PFAS as shown in Table S5.

#### 2.4 Quality control and quality assurance (QA/QC)

To verify the process of the nontarget procedure in Fig. 1, a PFAS standard mixture containing 39 compounds from 11 PFAS categories listed in Table S1 were prepared as a QC sample. The result showed that 92% (36 out of 39 compounds) were detectable through the processing of fragment-based nontarget analysis as detailed in Table S6. The specifics regarding the detection of mass

errors, fragments, neutral losses of the 39 compounds are provided in Table S7 and Table S8.

### 3 Results and discussion

#### 3.1 Nontarget analysis of PFAS and identified classes

Screening functional polar heads is crucial for identifying nontargeted PFAS without apparent fluorocarbon fragments and discovering various reaction products formed in the polar functional groups during the semiconductor manufacturing. Hence, we have streamlined the approach by summarizing the identified surfactant PFAS search through fragment and neutral loss screening of polar functional groups for the 12 classes with distinct polar functional groups, as shown in Table 1, serving as a valuable reference for nontarget analysis of PFAS. For miscellaneous perfluoroalkane sulfonamides (FASAs) and perfluoroalkane sulfonamido ethanols (FASEs; subclass 1d–1i and subclass 2 g–2 h of Table 2,

**Table 1** Summary of fragment and neutral loss (NL) screening from the fluorinated tail and polar head, respectively, in the study. Normal font subclasses recognized from both tail and head, bold subclasses only from headgroup, italicized subclass from tail

By tail By head	$[C_nF_{2n+1}]^-$	$[C_nF_{2n+1}O]^-$	$[C_nF_{2n-1}]^-$	$[C_nF_{2n-1}O]^-$	$[C_nF_{2n-3}]^-$	HF <sup>a</sup>	No prior fragments or NL from fluorinated tail
$[SO_2N]^-$	FASAAs	E-FASAAs E-FASAAs	H-FASAAs				FASAAs H-FASAAs
$[SO_2F]^-$	PFSAi N-Alkyl FASAAs						
$[SO_3]^-$	FASEEs			H <sub>2</sub> -E-PFSAs	H <sub>2</sub> -E-PFSAs	H-PFSAs n:2 FTSAs H <sub>2</sub> -E-PFSA	PFSAs
$[HSO_2]^-$	N-Alkyl FASAs FASEE mono-ol monoacids	E-FASEs	U-FASEs	E-H-FASEs U-E-FASEs			FASEs H-FASEs Miscellaneous FASEs FASAcALs FASAcAL hydrates/ hemiacetals
$[SO_2NC_2H_4O]^-$	FASEE mono-ol monoacids	E-FASEs	U-FASEs	H-E-FASEs U-E-FASEs			FASEs H-FASEs Miscellaneous FASEs
$[SO_2N(C_2H_4O)_2]^-$	FASEEs						H-FASEEs
CO <sub>2</sub> <sup>a</sup>	PFCAs U-E-PFCAs PFdiCAs		U-PFCAs U-E-PFCAs PFdiCAs	U-E-PFCAs	PFdiCAs		
CO <sub>2</sub> HF <sup>a</sup>	H-E-PFCAs H <sub>2</sub> -E-PFCAs	H-E-PFCAs	H-PFCAs	H-E-PFCAs			
C <sub>n</sub> H <sub>2n</sub> CO <sub>2</sub> <sup>ab</sup>	FASAAs FASPrAs N-Alkyl FASAAs FASEE diacids FASEE mono-ol monoacids	E-FASAAs	H-FASAAs				
X = SO <sub>3</sub> , CONH <sub>2</sub> <sup>a</sup>							Miscellaneous FASAAs Miscellaneous FASEs
No prior fragments and NL from head- group		E-PFCAs					

<sup>a</sup> Neutral losses from MS2 spectra

<sup>b</sup> The neutral loss from sulfonamido carboxylic acid is "C<sub>n</sub>H<sub>2n</sub>CO<sub>2</sub>", exemplified by sulfonamido acetic acid (CH<sub>2</sub>CO<sub>2</sub> 58.0055) and sulfonamido propanoic acid (C<sub>2</sub>H<sub>4</sub>CO<sub>2</sub> 72.0211)

**Table 2** Identified PFAS categorized by polar head class, subclass, compound number theoretical precursor ion, retention time (RT), confidence level (CL), and first report

Class	Subclass	Aberration	Compound number <sup>a</sup>	RT (min)	Theoretical precursor ion [M-H] <sup>-</sup> (m/z)	CL	First report <sup>d</sup>	
Sulfonamides- $\text{SO}_2\text{NH}_2$	1a	Perfluoroalkane sulfonamides (FASAs)	FBSA	1a-1	21.9	297.9590	1a	
	1b	Hydro-substituted perfluoroalkyl sulfonamides (H-FASAs)	H-FBSA	1b-1	10.7	279.9684	3a	V
	1c	Perfluoroalkyl ether sulfonamides (E-FASAs)	E-FBSA(1) E-FBSA(2)	1c-1 1c-2	25.9 27.4	313.9539 <sup>b</sup> 313.9539 <sup>b</sup>	2b 2b	V V
Miscellaneous sulfonamides - $\text{SO}_2\text{N}(\text{X})\text{H}$	1d	X: $\text{SO}_3\text{H}$	FBSA- $\text{SO}_3\text{H}$	1d-1	3.6	377.9158	2b	V
	1e	X: $\text{CONH}_2$	FBSA-Am	1e-1	8.7	340.9648	2b	V
	1f	X: $\text{CH}_2\text{CONH}_2$	FBSA-MeAm	1f-1	10.7	354.9804	3a	V
	1g	X: $\text{CH}_2\text{NO}_2$	FBSA-Me $\text{NO}_2$	1g-1	7.3	356.9597	3a	V
	1h	X: $\text{C}_3\text{H}_6\text{NO}_2$	FBSA-Pr $\text{NO}_2$	1h-1	8.8	384.9910 <sup>c</sup>	3a	V
	1i	X: $\text{CH}_2\text{N}_2\text{H}$	FBSA-diazene	1i-1	22.3	339.9808	3a	V
N-alkyl sulfonamides - $\text{SO}_2\text{N}(\text{R})\text{H}$	1j	N-methyl perfluoroalkane sulfonamides (MeFASAs) R= $\text{CH}_3$	MeFBSA	1j-1	36.8	311.9746	1a	
Sulfonamido ethanols - $\text{SO}_2\text{N}(\text{H})\text{CH}_2\text{CH}_2\text{OH}$	2a	Perfluoroalkane sulfonamido ethanols (FASEs)	FEtSE	2a-1	9.5	241.9916	2b	
			FPrSE	2a-2	18.5	291.9884	2b	
			FBSE	2a-3	30.0	341.9852	1b	
	2b	Hydro substituted perfluoroalkane sulfonamido ethanols (H-FASEs)	H-FBSE(1)	2b-1	15.8	323.9946 <sup>b</sup>	3a	V
			H-FBSE(2)	2b-2	19.1	323.9946 <sup>b</sup>	3a	V
	2c	Perfluoroalkyl ether sulfonamido ethanols (E-FASEs)	E-FBSE(1)	2c-1	33.9	357.9801 <sup>b</sup>	2b	V
			E-FBSE(2)	2c-2	34.3	357.9801 <sup>b</sup>	2b	V
			E-FBSE(3)	2c-3	35.1	357.9801 <sup>b</sup>	2b	V
2d	Hydrogen substituted perfluoroalkyl ether sulfonamido ethanols (E-H-FASEs)	H-E-FBSE	2d-1	21.4	339.9895	3a	V	
2e	Unsaturated perfluoroalkane sulfonamido ethanols (U-FASEs)	U-FBSE	2e-1	16.8	303.9884	3a	V	
2f	unsaturated perfluoroalkyl ether sulfonamido ethanols (U-E-FASEs)	U-E-FBSE	2f-1	23.8	319.9833	3a	V	
Miscellaneous sulfonamido ethanols - $\text{SO}_2\text{N}(\text{X})\text{CH}_2\text{CH}_2\text{OH}$	2g	X: $\text{SO}_3\text{H}$	FBSE- $\text{SO}_3\text{H}$	2g-1	17.8	421.9420	2b	V
	2h	X: $\text{CONH}_2$	FBSE-Am	2h-1	29.9	384.9910 <sup>c</sup>	2b	V
N-alkyl sulfonamido ethanols - $\text{SO}_2\text{N}(\text{R}')\text{CH}_2\text{CH}_2\text{OH}$	2i	N-methyl perfluoroalkane sulfonamido ethanols (MeFASEs) R= $\text{CH}_3$	MeFBSE	2i-1	35.2	416.0220 <sup>e</sup>	3a	
Sulfonamido diethanols - $\text{SO}_2\text{N}(\text{CH}_2\text{CH}_2\text{OH})_2$	3a	N,N-bis(2-hydroxyethyl) perfluoroalkane sulfonamides (FASEE diols)	FBSEE diol	3a-1	31.5	446.0325 <sup>e</sup>	1a	
	3b	Hydro-substituted FASEE diol (H-FASEE diols)	H-FBSEE	3b-1	16.9	428.0420 <sup>e</sup>	2b	V

**Table 2** (continued)

Class	Subclass	Aberration	Compound number <sup>a</sup>	RT (min)	Theoretical precursor ion [M-H] <sup>-</sup> (m/z)	CL	First report <sup>d</sup>	
Sulfonamido carboxylic acids -SO <sub>2</sub> NH(CH <sub>2</sub> ) <sub>n</sub> COOH	4a	perfluoroalkane sulfonamido acetic acids (FASAAs)	FBSAA	4a-1	15.5	355.9645 <sup>c</sup>	1a	V
			Headgroup isomer of FBSAA	4a-2	9.93	355.9645 <sup>c</sup>	3a	
	4b	Hydro-substituted FASAAs (H-FASAAs)	H-FBSAA	4b-1	7.3	337.9739	3a	V
	4c	Perfluoroalkyl ether sulfonamido acetic acids (E-FASAAs)	E-FBSAA(1)	4c-1	18.7	371.9594 <sup>b</sup>	3a	V
			E-FBSAA(2)	4c-2	19.7	371.9594 <sup>b</sup>	3a	V
4d	N-methyl FASAAs (N-MeFASAAs)	MeFBSAA	4d-1	20.4	369.9812 <sup>c</sup>	1a		
4e	Perfluoroalkane sulfonamido propanoic acids (FASPrAs)	FBSPrA	4e-1	19.1	369.9812 <sup>c</sup>	2b	V	
Sulfonamido diacetic acids -SO <sub>2</sub> N(CH <sub>2</sub> COOH) <sub>2</sub>	5a	perfluoroalkane sulfonamido diacetic acids (FASEE diacids)	FBSEE diacid	5a-1	5.8	413.9699	2b	
N-ethylhydroxyl sulfonamido acetic acids -SO <sub>2</sub> N(CH <sub>2</sub> CH <sub>2</sub> OH)(CH <sub>2</sub> COOH)	6a	N-(2-hydroxyethyl) perfluoroalkane sulfonamido acetic acids (FASEE mono-ol monoacid)	FBSEE mono-ol monoacid	6a-1	17.1	399.9907	2b	
Sulfonamido acetaldehyde -SO <sub>2</sub> N(H)CH <sub>2</sub> COH	7	Perfluoroalkane sulfonamido acetaldehyde (FASALs, keto and enol form)	FBSAcAL(1)	7a-1	13.0	339.9695 <sup>c</sup>	3a	V
			FBSAcAL(2)	7a-2	30.0	339.9695 <sup>c</sup>	3a	V
Sulfonamido acetaldehyde hydrate/hemiacetal -SO <sub>2</sub> N(H)CH <sub>2</sub> C(OH)(OR)H	8a	Perfluoroalkane sulfonamido acetaldehyde hydrate (R=H)	FBSAcAL hydrate	8a-1	30.0–32.6	357.9801	2b	V
	8b	Perfluoroalkane sulfonamido acetaldehyde hemiacetal (R=CH <sub>3</sub> )	FBSAcAL hemiacetal	8b-1	33.2	371.9958	2b	V
Carboxylic acid -COOH	9a	Perfluoroalkyl carboxylic acids (PFCAs)	TFA	9a-1	1.4	112.9856	1a	
			PFPrA	9a-2	2.7	162.9825	1a	
			PFBA	9a-3	4.4	212.9792	1a	
			PFPeA	9a-4	8.2	262.9760	1a	
			PFHxA	9a-5	15.9	312.9728	1a	
			PFHpA	9a-6	25.5	362.9696	1a	
			PFOA	9a-7	35.3	412.9664	1a	
			PFNA	9a-8	45.9	462.9632	1a	
			PFDA	9a-9	54.8	512.9600	1a	
			PFUdA	9a-10	63.1	562.9568	1a	
U-E-PFPeA(1) U-E-PFPeA(2)	9b	Unsaturated PFCAs (U-PFCAs)	U-PFHxA	9b-1	10.5	274.9760	3a	

**Table 2** (continued)

Class	Subclass	Aberration	Compound number <sup>a</sup>	RT (min)	Theoretical precursor ion [M-H] <sup>-</sup> (m/z)	CL	First report <sup>d</sup>	
U-E-PFHxA(1)	9c	Unsaturated-E-PFCAs (U-E-PFCAs)	U-E-PFBA	9c-1	3.2	190.9773	3a	
			U-E-PFPeA(1)	9c-2	3.3	240.9741 <sup>b</sup>	3a	
			U-E-PFPeA(2)	9c-3	6.4	240.9741 <sup>b</sup>	3a	
			U-E-PFHxA(1)	9c-4	3.7	290.9709 <sup>b</sup>	3a	
			U-E-PFHxA(2)	9c-5	5.8	290.9709 <sup>b</sup>	3a	
			U-E-PFHxA(3)	9c-6	11.1	290.9709 <sup>b</sup>	3a	
	9d	Hydro-substituted PFCAs (H-PFCAs)	H-PFBA	9d-1	3.2	194.9886	3a	
			H-PFPeA	9d-2	4.7	244.9854	3a	
			H-PFHxA	9d-3	9.4	294.9822	3a	
	9e	Hydro-substituted E-PFCAs (H-E-PFCAs)	H-E-PFPrA	9e-1	1.9	160.9867	3a	
			H-E-PFBA(1)	9e-2	3.1	210.9835 <sup>b</sup>	3a	
			H-E-PFBA(2)	9e-3	3.8	210.9835 <sup>b</sup>	3a	
			H-E-PFBA(3)	9e-4	9.8	210.9835 <sup>b</sup>	3a	
	9f	Multihydro-substituted E-PFCAs (H <sub>n</sub> -E-PFCAs)	H <sub>2</sub> -E-PFBA	9e-5	1.8	192.9930	3a	
	Dicarboxylic acid -(COOH) <sub>2</sub>	10a	Perfluoroalkyl ether carboxylic acids (E-PFCAs)	E- PFPrA	9f-1	3.4	178.9773	3a
				E- PFBA	9f-2	5.8	228.9741	3a
				E- PFPeA	9f-3	10.1	278.9709	3a
PFdiCA(C3)				10a-1	1.0	138.9848	3c	
PFdiCA(C4)				10a-2	1.1	188.9816	2c	
PFdiCA(C5)				10a-3	1.1	238.9785	2c	
Sulfonic acid -SO <sub>3</sub> H	11a	Perfluoroalkane sulfonic acids (PFSAs)	TFMS	11a-1	1.8	148.9526	1a	
			PFBS	11a-2	9.8	298.9430	1a	
	11b	Hydro substituted PFSAs (H-PFSAs)	H-PFETs	11b-1	1.9	180.9588	3a	
			H-PFPrS	11b-2	3.6	230.9556	3a	
			H-PFBS	11b-3	5.2	280.9524	3a	
	11c	Hydro substituted perfluoroalkyl ether sulfonic acids (H <sub>n</sub> -E-PFSAs)	H <sub>2</sub> -E-PFTS	11c-1	1.3	178.9631	3a	
			H <sub>2</sub> -E-PFPrS	11c-2	2.6	228.9599	3a	
	11d	Fluorotelomer sulfonic acid	6:2FTSA	11d-1	33.9	426.9679	1a	
Sulfinic acids -SO <sub>2</sub> H	12a	Perfluoroalkyl sulfinic acids (PFSiA)	PFBSi	12a-1	11.5	282.9481	1a	

<sup>a</sup> Compound number is made up of the subclass and serial number. For each chemical structure, please refer to Table S9 of SM

<sup>b</sup> The presence of structural isomers varied in the fluorinated chain

<sup>c</sup> The presence of structural isomers varied in the polar functional head

<sup>d</sup> The structures of these compounds have been firstly identified

<sup>e</sup> The precursor ion was an acetate adduct [M + CH<sub>3</sub>COO]<sup>-</sup>

with further information in Table S9), the prominent signals at 297.9590, representing  $[C_4F_9SO_2N]^-$ , and 341.9852, representing  $[C_4F_9SO_2NC_2H_4OH]^-$ , suggest that these ions likely retain the original structures of FBSA and FBSE during fragmentation. Hence, the neutral loss between  $[M-H]^-$  and their associated fragment ( $[C_4F_9SO_2NH]^-$  for FBSA and  $[C_4F_9SO_2NC_2H_4OH]^-$  for FBSE), would be practical to identify these series of headgroups, despite potential variations at the fluorinated tail end. This approach uniquely emphasizes the neutral loss of segments such as  $SO_3$ ,  $CONH$ ,  $CH_3OH$ , and  $H_2O$  for miscellaneous FASAs and FASEs, underscoring its novelty in identifying reaction products

reported for the first time. The initial proposed structure belonging to miscellaneous FASAs and miscellaneous FASEs are provided in Fig. 2. In addition, our study leads the way in developing neutral loss screens for  $CO_2$ ,  $HFCO_2$ ,  $C_nH_{2n}CO_2$ , etc., serving as indicators to distinguish classes such as carboxylic acid, dicarboxylic acid, and sulfonamido carboxylic acid, each characterized by terminal carboxylate structures. A list of the 83 identified PFAS and their formula, retention time (RT), precursor ion, and theoretical  $m/z$  are provided in Table 2. The following is a discussion of the identified results for the 12 classes with distinct polar functional groups.

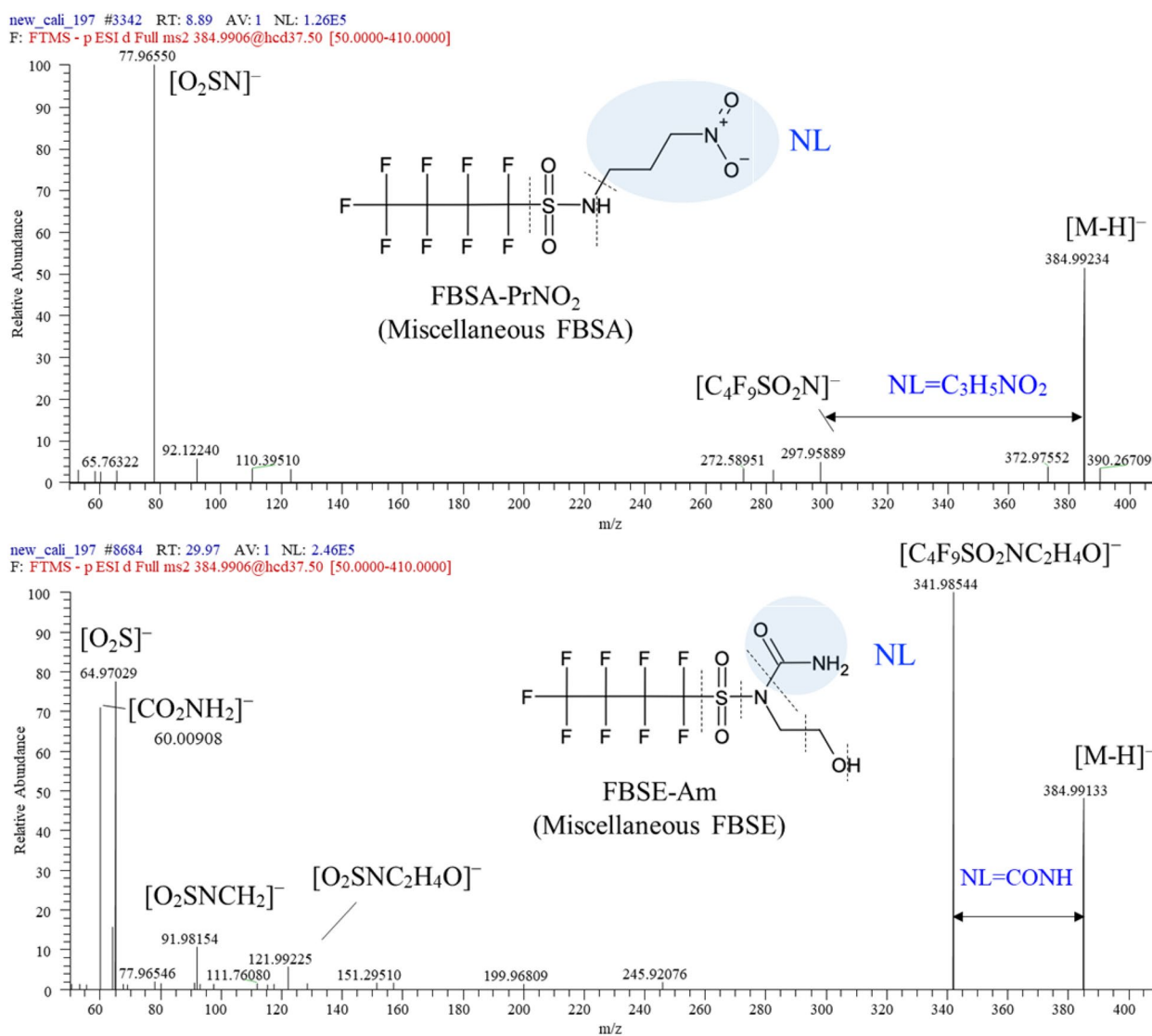


**Fig. 2** FBSA-PrNO<sub>2</sub> and FBSE-Am are polar-head isomers, presenting the subclass of sulfonamide and sulfonamido ethanol respectively



### 3.1.1 Class 1 Sulfonamides

By searching for  $[\text{SO}_2\text{N}]^-$  fragment searching and excluding substances lacking fluorine based on isotopic formulas based on the workflow in Fig. 1, we identified the predominant FASAs and various FASA series chemicals, resulting in the detection of 9 subclasses (subclass 1a-1i of Table 2). Among them, 3 subclasses (1a-1c) displayed variations in the fluoroalkyl chain but had a polar head of  $-\text{SO}_2\text{NH}_2$ . This class exhibits a unique characteristic fragment,  $[\text{SO}_2\text{N}]^-$  (77.9644), which is observed in FBSA, hydro-substituted FBSA (H-FBSA), and ether FBSA (E-FBSA). Notably, no obvious fragmentations from the fluoroalkyl tail were detected during screening, suggesting that  $[\text{SO}_2\text{N}]^-$  is a feasible screening tool for identifying these subclasses. In Fig. S3, due to the lack of fragments to determine the position of the hydrogen, the CL for H-FBSA remained at 3a. Conversely, E-FBSA, observed with two isomers in this study, was identified by its distinct ether fragments  $[\text{CF}_3\text{O}]^-$  (84.9907) and  $[\text{C}_2\text{F}_5\text{O}]^-$  (134.9875). Accordingly, their proposed structures were presented in Figs. S4a and S4b, classifying them to CL 2b based on Charbonnet's classification [26].

The remaining 6 subclasses (1d-1i) featured a fixed fluoroalkyl chain as perfluorobutane but showed variations in the functional group as  $-\text{SO}_2\text{N}(\text{X})\text{H}$ . The miscellaneous FASAs with the structure  $\text{C}_4\text{F}_9\text{SO}_2\text{NHX}$  (X:  $\text{SO}_3\text{H}$ ;  $\text{CONH}_2$ ;  $\text{CH}_2\text{CONH}_2$ ;  $\text{CH}_2\text{NO}_2$ ;  $\text{C}_3\text{H}_6\text{NO}_2$ ;  $\text{CH}_2\text{N}_2\text{H}$ , subclass 1d-1i) were identified with the fragment of  $[\text{SO}_2\text{N}]^-$  (77.9644). Figures 2 and S5 illustrate a neutral loss of  $\text{C}_3\text{H}_5\text{NO}_2$  between  $[\text{C}_4\text{F}_9\text{SO}_2\text{N}]^-$  (297.9589) and  $[\text{M}-\text{H}]^-$ , representing a novel screening approach for miscellaneous FASAs with various headgroup. Notably, in the presence of substances with N-alkyl substitutions, the dominant fragments  $[\text{SO}_2]^-$  (63.9625) and  $[\text{SO}_2\text{H}]^-$  (64.9697) were observed, along with the weak fragment  $[\text{SO}_2\text{F}]^-$  (82.9603). N-Methyl FBSA (MeFBSA) was identified in the effluents of WWTP I and WWTP II (Fig. S6a). It was subsequently confirmed by an authentic standard of MeFBSA, matching both in RT and MS2 spectra, resulting in setting the CL to 1a (Fig. S6b). To the best of our knowledge, 9 identified PFAS (including 2 E-FBSA isomers) of these subclasses have been reported for the first time, as shown in Table 2. Remarkably, while previous studies illustrated that fluorotelomer sulfonamides detected with the  $[\text{H}_2\text{NSO}_2]^-$  fragment [20, 27], and the hydrogens of the  $[\text{H}_2\text{NSO}_2]^-$  fragment is attributed to the substantial presence of hydrogens in the fluorotelomer.

### 3.1.2 Class 2 Sulfonamido ethanols

The class has a structure where sulfonamido is linked to a hydroxyethyl group, and its main characteristic fragments are  $[\text{SO}_2\text{NC}_2\text{H}_4\text{O}]^-$  (121.9912) and  $[\text{SO}_2\text{NCH}_2]^-$  (91.9806). By conducting these fragments searching

and subsequently excluding substances lacking fluorine based on isotopic formulas, we identified the predominant FASEs and miscellaneous FASE series, resulting in the detection of 8 subclasses (2a-2 h). Among them, 6 subclasses (2a-2f) displaying variations in the fluoroalkyl chain were effectively identified, including FBSE, hydrogen-substituted FBSE (H-FBSE), perfluorobutyl ether sulfonamido ethanol (E-FBSE), unsaturated FBSE (U-FBSE), hydro-substituted E-FBSE (H-E-FBSE), and unsaturated E-FBSE (U-E-FBSE). Figure S7 displays the MS2 spectrum and proposed structure of H-FBSE. The CL for H-FBSE remains at 3a due to uncertainties in identifying the position of hydrogen. Next, three isomers of E-FBSE were identified and three characteristic peaks from fragments  $[\text{CF}_3\text{O}]^-$ ,  $[\text{C}_3\text{F}_7\text{O}]^-$ , and  $[\text{C}_2\text{F}_5\text{O}]^-$  were observed by chromatography, and their structures were proposed (Figs. S8a-S8c) with a CL of 2b. The longer RT (35.1 min) of the E-FBSE isomer indicates increased symmetry in the alkyl structure, consistent with the proposed structure. The presence of H-E-FBSE with the specific fluoroalkyl ether fragment  $[\text{C}_2\text{F}_3\text{O}]^-$  (96.9907, 0.72 ppm) was indicative of the loss of HF from  $[\text{C}_2\text{F}_4\text{HO}]^-$  (116.9971, 1.54 ppm). U-FBSE with the fragment  $[\text{C}_4\text{F}_7]^-$  (180.9896, 0.99 ppm) was detected. We proposed a CL of 3a due to the lack of further information to determine the position of the double bond. U-E-FBSE with the specific fragments  $[\text{C}_3\text{F}_5]^-$  (130.9928, 1.91 ppm) and  $[\text{C}_4\text{F}_7\text{O}]^-$  (196.9850, 3.79 ppm) were detected, which suggested the position of the oxygen atom (Fig. S9). However, the position of the unsaturated bond remained uncertain, so the CL was set to 3a. To the best of our knowledge, 5 subclasses (subclasses 2b-2f) of FASEs with various fluoroalkyl chains have been reported for the first time (Table 2). In addition, miscellaneous FBSEs with the structure  $\text{C}_4\text{F}_9\text{SO}_2\text{N}(\text{X})(\text{C}_2\text{H}_4\text{OH})$  (X:  $\text{SO}_3\text{H}$ ; X:  $\text{CONH}_2$ ) were detected in subclasses 2 g and 2 h, identified through characteristic fragment  $[\text{SO}_2\text{NC}_2\text{H}_4\text{O}]^-$  (121.9912) screening. Notably, subclasses 2 g and 2 h could be detected through neutral loss screening of  $\text{SO}_3$  and  $\text{CONH}$  (Fig. S10).

To explore subclass (2i) of N-alkyl FASE, authentic standards of MeFOSE and EtFOSE were used to comprehend characteristic MS2 spectra of this subclass. Both MeFOSE and EtFOSE displayed an acetate adduct  $[\text{M}+\text{CH}_3\text{COO}]^-$ . In N-alkyl FASE, we did not observe the  $[\text{SO}_2\text{NC}_2\text{H}_4\text{O}]^-$  (121.9912) and  $[\text{SO}_2\text{NCH}_2]^-$  (91.9806) fragments; only  $[\text{CH}_3\text{COO}]^-$  (59.0139) appeared. Therefore, we screened the acetate adduct of N-methyl perfluorobutane sulfonamido ethanols (MeFBSE) (416.0220), and in sample no. 190, we identified a suspect peak of MeFBSE revealing fragments of  $[\text{SO}_2\text{NC}_2\text{H}_4\text{O}]^-$  (121.9925),  $[\text{SO}_2\text{H}]^-$  (64.9703) and  $[\text{CH}_3\text{COO}]^-$  (59.0141) at RT 35.8 min (Fig. S11a).

After obtaining the authentic standard of MeFBSE, we found that while the RT and MS1 spectra matched, the MS2 spectrum did not resemble that of the sample (Fig. S11b). As a result, MeFBSE is classified as CL 3a due to the presence of only one fragment corresponding to the headgroup, consistent with the identification criteria outlined in Table S5. However, due to lacked information for the identification of MeFBSE, further study is needed. Remarkably, fluorotelomer sulfonamido ethanol, such as 6:2 FTSAm-EtOH, which was identified by other researchers are detected, contains the  $[\text{SO}_2\text{NC}_2\text{H}_4\text{O}]^-$  (121.9912) fragment [27]. This fragment, elucidated as  $[\text{SO}_2\text{NC}_2\text{H}_4\text{O}]^-$  (121.9912), remains unaffected by the functional fluoroalkyl chain, including fluorotelemer, serving as a unique indicator of the class of sulfonamido ethanol.

### 3.1.3 Class 3 Sulfonamido diethanol

FBSEE diol was identified and detected in the form of an acetate adduct  $[\text{M}+\text{CH}_3\text{COO}]^-$ ,  $[\text{M}-\text{H}]^-$ , a formate adduct  $[\text{M}+\text{HCOO}]^-$ , and a dimer ion  $[2\text{M}-\text{H}]^-$ , in the order of their observed intensities (Fig. S12). This structure exhibited characteristic fragments, including  $[\text{SO}_2\text{N}(\text{C}_2\text{H}_4\text{O})_2]^-$ ,  $[\text{SO}_2\text{N}(\text{C}_2\text{H}_4\text{O})\text{CH}_2]^-$ , and  $[\text{SO}_2\text{NC}_2\text{H}_4\text{O}]^-$ . Additionally, the high-intensity  $[\text{SO}_3]^-$  fragment serves as a confirming marker. FBSEE diol exhibited a weak characteristic fragment of the fluorobutyl fragment  $[\text{C}_4\text{F}_9]^-$ , highlighting the feasibility of the screening method based on its functional group, as shown in Figs. S13a and S13b. Hydrogen-substituted FBSEE diol (H-FBSEE diol) was detected with an acetate adduct and the unique fragment  $[\text{O}_2\text{SN}(\text{C}_2\text{H}_4\text{O})_2]^-$  (166.0174, -2.16 ppm) for the first time. The CL was set to 3a due to insufficient data to determine the position of hydrogen.

### 3.1.4 Class 4 Sulfonamido carboxylic acid

This subclass features a structure with sulfonamido linked to a carboxylic acid group, releasing the carboxylic acid group during collision and producing characteristic fragments such as  $[\text{SO}_2\text{N}]^-$  (77.9656) and  $[\text{SO}_2\text{F}]^-$  (82.9610). A precursor ion at 355.9654, with a neutral loss of  $\text{CH}_2\text{CO}_2$  (8.31 ppm), was identified as perfluorobutane sulfonamido acetic acid (FBSAA) (Fig. S14a) and confirmed by its authentic standard at CL1a (Fig. S14b). The features observed at 337.9743 in Fig. S15, which include the detection of neutral loss of  $\text{CH}_2\text{CO}_2$ , fragments such as  $[\text{SO}_2\text{N}]^-$  and  $[\text{C}_4\text{F}_7]^-$ , and the formula inferred through isotopic pattern matching as  $\text{C}_6\text{H}_5\text{F}_8\text{O}_4\text{SN}$  (mass tolerance 1.26 ppm, within 5 ppm), were further suggested to represent hydrogen-substituted FBSAA (H-FBSAA). Additionally, the features observed at 369.9805 in Fig. S16a, exhibiting neutral loss of  $\text{CH}_2\text{CO}_2$ , along with fragments such as  $[\text{SO}_2\text{F}]^-$  and  $[\text{C}_4\text{F}_9]^-$ , and the formula inferred through

isotopic pattern matching, were proposed to represent MeFBSAA. This identification was further supported by matching the RT and MS2 spectra of the authentic standards (Fig. S16b). Furthermore, features as 371.9594 are proposed as perfluorobutyl ether sulfonamido acetic acid (E-FBSAA), which has two structural isomers, was separated with the column at RT of 18.7 and 19.7 min. Fragments of fluoroether  $[\text{CF}_3\text{O}]^-$  and  $[\text{C}_2\text{F}_5\text{O}]^-$  were observed and providing the position of oxygen for the CL at 2b. These findings have been summarized in Table 1 to serve as a reference for assisting in the identification of nontarget PFAS. Notably, a structural isomer of MeFBSAA, was identified for the first time as perfluorobutane sulfonamido propanoic acid (FBSPrA) (Fig. S17). The neutral loss of  $\text{C}_2\text{H}_4\text{CO}_2$  released from collision indicates propanoic acid. The presence of only  $[\text{SO}_2\text{F}]^-$  (82.9603) fragments, not  $[\text{SO}_2\text{N}]^-$  (77.9644), serves as a distinguishing rule between perfluoroalkane sulfonamido acetic acids (FASAAs) and N-alkyl FASAAs. Notably, the distinct neutral loss of  $\text{CH}_2\text{CO}_2$  might be affected by the significant presence of hydrogens in the fluorotelomer, resulting in the neutral loss of HF instead [27]. However, the fluorotelomer series was not detected in this study; additional information for exclusion purposes is provided.

### 3.1.5 Class 5 sulfonamido diacetic acid

The MS2 spectrum of sulfonamido diacetic acid shows two pairs of neutral losses of  $\text{CH}_2\text{CO}_2$ , indicating the presence of the diacetic acid structure. The main characteristic fragment was  $[\text{SO}_2\text{F}]^-$  (82.9603), while the intensity of  $[\text{SO}_2\text{N}]^-$  (77.9644) was notably weak. Perfluorobutane sulfonamido diacetic acid was identified with CL to 2b [10].

### 3.1.6 Class 6 N-hydroxyethyl sulfonamido acetic acid

The substance with the precursor ion 399.9903 was identified by the specific fragment of  $[\text{O}_2\text{SNC}_2\text{H}_4\text{O}]^-$  (121.9912). An obvious fragment 341.9852 was referred to as the FBSE fragment. The difference between 341.9852 and 399.9903 represents the neutral loss of  $\text{CH}_2\text{CO}_2$ . Consequently, we referred to this substance as N-(2-hydroxyethyl) FBSAA (FBSEE mono-ol monoacid) at CL 2b [10].

### 3.1.7 Class 7 Sulfonamido acetaldehyde

The class with the structure where sulfonamido linked to acetaldehyde. A precursor ion  $[\text{C}_6\text{H}_3\text{F}_9\text{NO}_3\text{S}]^-$  was observed with the RT of 13.1 min and the RT of 30.1 min, identified for the first time as perfluorobutane sulfonamido acetaldehyde in its enol form and keto form (Figs. S18a and S18b). The enol form illustrated plenty of fragments ( $[\text{SO}_2\text{N}]^-$ ,  $[\text{SO}_3]^-$ ,  $[\text{SO}_2\text{F}]^-$ ,  $[\text{SO}_2\text{NCH}_2\text{CHO}]^-$ ),

while the keto form showed simple fragments ( $[\text{SO}_2]^-$  and  $[\text{SO}_2\text{H}]^-$ ).

**3.1.8 Class 8 Sulfonamido acetaldehyde hydrate/hemiacetal**  $[\text{C}_6\text{H}_5\text{F}_9\text{NO}_4\text{S}]^-$  (357.9812, 2.99 ppm) was observed with a neutral loss of  $\text{H}_2\text{O}$  which was identified as perfluoroalkane sulfonamido acetaldehyde hydrate, as water adds to the carbonyl function of acetaldehydes (Fig. S19). Moreover,  $[\text{C}_7\text{H}_7\text{F}_9\text{NO}_4\text{S}]^-$  (371.9954, -0.89 ppm) was detected with a neutral loss of  $\text{CH}_3\text{OH}$ , which indicated the production of additional reaction of methanol to acetaldehyde. Hydrates and hemiacetals are the products of addition reactions of oxygen-based nucleophiles, such as water and methanol, to aldehydes, which have been reported for the first time.

### 3.1.9 Class 9 carboxylic acid

Integrating  $\text{CO}_2$  neutral loss into the nontarget approach improves the identification of carboxylic acid-containing compounds, revealing their collision characteristics in the collision activated dissociation cell, including subclasses 9a-9e, encompassing perfluoroalkyl carboxylic acids (PFCAs), unsaturated PFCAs (U-PFCAs), perfluoroalkyl ether carboxylic acids (E-PFCAs), unsaturated-E-PFCAs (U-E-PFCAs), hydro-substituted PFCAs (H-PFCAs), and hydro-substituted E-PFCAs (H-E-PFCAs). The MS2 spectrum of U-E-PFCA(C6) is shown in Fig. S20. The detection of neutral loss as  $\text{CO}_2$  alongside other fluorinated fragments ( $[\text{C}_3\text{F}_5]^-$ ,  $[\text{C}_4\text{F}_7]^-$ ,  $[\text{C}_5\text{F}_9\text{O}]^-$ ,  $[\text{C}_6\text{F}_9\text{O}_3]^-$ ) and confirmation through isotope pattern matching with a formula of  $\text{C}_6\text{F}_9\text{O}_3\text{H}$  allowed us to propose the structure of U-E-PFCA (C6) as CL 3a, due to uncertainties regarding the position of the unsaturated bond. In addition, H-PFCAs, H-E-PFCAs and  $\text{H}_n$ -E-PFCAs (subclasses 9d and 9e) produced neutral loss of  $\text{CO}_2\text{HF}$ , which was derived through the combination of  $\text{CO}_2$  and HF, with HF originating from the hydrogen-substituted fluoroalkyl chain, as their MS2 spectrum are shown in Figs. S21 and S22 for H-PFCA(C4) and  $\text{H}_2$ -E-PFCA(C4), respectively. Contrarily, achieving a neutral loss of  $\text{CO}_2$  in the PFCA series typically requires the presence of  $[\text{M}-\text{H}]^-$  as a precursor ion and  $[\text{M}-\text{H}-\text{CO}_2]^-$  as a product ion. However, due to E-PFCA's inherent susceptibility to in-source collision-induced dissociation [21, 28, 29],  $\text{CO}_2$  can be lost, resulting in the formation of  $[\text{M}-\text{H}-\text{CO}_2]^-$  as the precursor ion. Subsequently, within the collision chamber, C-O cleavage generates  $[\text{C}_x\text{F}_y\text{O}_z]^-$  fragments. Thus, there is no neutral loss of  $\text{CO}_2$  between the precursor ion and the production ion. This occurrence was observed during our QC sample testing with HFPO-DA (GenX), where the precursor ion was identified as  $[\text{M}-\text{H}-\text{CO}_2]^-$  (284.9779) in Table S7 and the product ion as  $[\text{C}_3\text{F}_7\text{O}]^-$  (184.9842) in Table S8, precluding a neutral loss of 44. Therefore,

E-PFAC detection relies on  $[\text{C}_n\text{F}_{2n+1}\text{O}]^-$  fragments and isotope pattern matching rather than  $\text{CO}_2$  screening. This aspect is also outlined in Table 1, highlighting the importance of simultaneously scanning the fluorinated tail and polar head to enhance the effectiveness of fragment-based nontarget analysis.

### 3.1.10 Class 10 dicarboxylic acid

Perfluoroalkyl dioic acids (PFdiCA, C3-C8) are comprised of the functional group of dicarboxylic acid. PFdiCA (C3-C5) exhibited a neutral loss of  $\text{CO}_2$ ; PFdiCA (C6-C8) lacked the detection of neutral loss of  $\text{CO}_2$ , presumably due to their low abundance in the samples. The fragment-based fluoroalkyl chain as  $\text{C}_n\text{F}_{2n-1}$  and the isotopic pattern of fluorine could be alternatives to identify this subclass. Fragments of  $[\text{C}_2\text{F}_3]^-$ ,  $[\text{C}_3\text{F}_5]^-$ ,  $[\text{C}_4\text{F}_7]^-$ ,  $[\text{C}_5\text{F}_9]^-$ , and  $[\text{C}_6\text{F}_{11}]^-$  ( $[\text{C}_n\text{F}_{2n-1}]^-$ ) were detected in the spectrum of PFdiCA (C4 to C8) respectively. The fragments  $[\text{C}_2\text{HF}_2\text{O}_2]^-$ ,  $[\text{C}_3\text{HF}_4\text{O}_2]^-$ ,  $[\text{C}_4\text{HF}_6\text{O}_2]^-$  were detected by the neutral loss of  $\text{CO}_2$  from  $[\text{M}-\text{H}]^-$  of PFdiCA(C3-C5).

### 3.1.11 Class 11 sulfonic acid

Perfluoroalkyl sulfonic acids (PFSAs, subclass 11a, C1 and C4) and hydrogen-substituted PFSA (H-PFSA, subclass 11b, C2-C4) were distinguished by the presence of  $[\text{SO}_3]^-$  and  $[\text{SO}_3\text{F}]^-$ . In the case of multi-hydrogen-substituted perfluoroalkyl ether sulfonic acids ( $\text{H}_2$ -E-PFSA, C4), the dominant fragments of polar head shifted from  $[\text{SO}_3]^-$  to  $[\text{HSO}_3]^-$ . Additionally, for the subclasses with hydrogen-substituted PFSAs, such as H-PFSA (C2, C3) and  $\text{H}_2$ -E-PFSA (C4), a neutral loss of HF was observed (Fig. S23).

### 3.1.12 Class 12 Sulfinic acid

Perfluorobutyl sulfinate (PFBSi) was identified with clear fragments of  $[\text{SO}_2\text{F}]^-$  as the specific feature of sulfinic acid. It was further confirmed with an authentic standard based on the RT and the MS2 spectrum. Perfluoroalkane sulfinic acids, arising from the degradation of commercial precursor compounds containing the  $\text{C}_n\text{F}_{2n+1}\text{SO}_2\text{N}$  moiety, may act as degradation by-products of fluorosurfactants in 3 M foam [10, 30].

## 3.2 Byproducts from chemical formulation

Two primary methods for PFAS production are the electrochemical fluorination (ECF) process, favored by 3 M [31], and the telomerization process, employed by DuPont [32]. The ECF process generates byproducts, along with both shorter and longer PFAS, with a higher prevalence of branched PFAS, while the telomerization process primarily yields linear PFAS [33]. In our previous study on semiconductor wastewater, FBSE was found at concentrations

ranging from 0.883 to 482  $\mu\text{g L}^{-1}$ , while perfluoropropane sulfonamido ethanol (FPrSE) and perfluoroethane sulfonamido ethanol (FEtSE) were detected at semi-concentrations of n.d. to 0.037  $\mu\text{g L}^{-1}$  and n.d. to 0.014  $\mu\text{g L}^{-1}$ , respectively [10]. FBSE is associated with 3 M's electronic surfactant 4200 [7], which is added to buffered hydrofluoric acid for etching solutions in semiconductor manufacturing to enhance wetting properties and improving pattern quantity performance. In this study, we reported several FBSE derivatives with varying fluoroalkyl chain in wastewater, including those with backbones containing oxygen as ether (E-FBSE), those with backbones containing unsaturated bonds (U-FBSE), and those with hydrogen-substituted F as polyfluoroalkyl chains (H-FBSE). The varied RTs of these substances compared to that of FBSE are as follows: H-FBSE (15.8–19.1 min) < U-FBSE (16.9 min) < H-E-FBSE (21.1 min) < U-E-FBSE (23.3 min) < FBSE (29.9 min) < E-FBSE (33.8–34.9 min). The use of a reversed-phase C18 column for analysis indicates that, in terms of polarity, only E-FBSE was less polar than FBSE, while the others were much more polar, resulting in faster elution. The aforementioned FBSE derivative series were found as impurities in the authentic standard of FBSE. Their relative area proportions, shown in Table 3 in descending order, were as follows: FPrSE (0.21%), E-FBSE (0.10%), H-FBSE (0.095%), FBSAA (0.036%), U-E-FBSE (0.033%), FEtSE (0.014%), U-FBSE (0.007%), headgroup isomer of FBSAA (0.002%), and H-E-FBSE (0.001%), contributing to a total of approximately 0.5%. In addition, H-FBSA (0.01%) and E-FBSA (0.06%) are included in the authentic

standard of FBSA, while H-FBSEE diol (0.4%) is included in the authentic standard of FBSEE diol, as shown in Table 3. The presence of FBSE derivatives, FBSA derivatives, and FBSEE diol derivatives in the authentic standard suggests that these derivative series detected in wastewater may originate from the byproducts of chemical formulations, like 3 M's electronic surfactant 4200, which contains FBSE as a primary component in semiconductor production. However, these byproducts may arise from transformation processes during manufacturing and among the treatment of wastewater, including the elimination of HF to produce unsaturated PFAS [34, 35] and defluorination leading to hydrogen-substituted PFAS under photoelectrochemical processes [36]. Additionally, under biotic metabolism, alcohol oxidation can lead to the formation of carboxylic acids through hydration and oxidation processes [10, 37], with further discussion below. This suggests that in wastewater treatment, using hydrophobic interaction separation methods such as activated carbon adsorption may lead to lower removal efficiency for these polar substances, decreasing susceptibility to adsorption removal [38]. When discharged from wastewater treatment plants, the environmental distribution of these substances may differ significantly due to their distinct properties. Notably, the semiconductor industry encompasses various suppliers, including those for logic integrated circuits, dynamic random-access memory devices, solid-state drives, photodiodes, photo-imaging sensors, and more. Generally, plants A, B, C, and D primarily manufacture similar products, while plant E specializes in a different product line. We discovered

**Table 3** List of impurities in authentic standards of FBSE, FBSA, and FBSEE diol

Characteristics	Compound	Compound number <sup>a</sup>	The relative peak area (%) <sup>b</sup>
Standard	FBSE	2a-3	99.50
Impurities in the standard	FPrSE	2a-2	0.211
	E-FBSE	2c-1, 2c-2, 2c-3	0.104
	H-FBSE	2b-1, 2b-2	0.095
	FBSAA	4a-1	0.036
	U-E-FBSE	2f-1	0.033
	FEtSE	2a-1	0.014
	U-FBSE	2e-1	0.007
	Headgroup isomer of FBSAA	4a-2	0.002
	H-E-FBSE	2d-1	0.001
Standard	FBSA	1a-1	99.93
Impurities in the standard	E-FBSA	1c-1 & 1c-2	0.062
	H-FBSA	1b-1	0.012
Standard	FBSEE diol	3a-1	99.57
Impurities in the standard	H-FBSEE diol	3b-1	0.403

<sup>a</sup> Compound number is made up of the subclass and serial number. For each chemical structure, please refer to Table S9 of SM

<sup>b</sup> The relative peak area (%) = Peak area of compound / Sum of peak areas of all compounds

that wastewater from plants A, B, C, and D contained significant quantities of FBSE, FBSA, and FBSEE diol, along with various fluoroalkyl sulfonamido derivatives such as E-FBSA, H-FBSE, and U-E-FBSE. In contrast, wastewater from plant E, which manufactures different products from plants A, B, C, and D, showed no presence of sulfonamido derivatives. This observation could serve as a distinguishing characteristic for identifying different production lines.

### 3.3 Reaction products

Due to the intricate nature of semiconductor processes, among the 12 prominent semiconductor industries in South Korea, 11 utilize 135 chemical constituents [39]. These include sulfuric acid, chromic acid, tetramethyl ammonium hydroxide, ethylene oxide, potassium dichromate, isopropanol, and formaldehyde, 33% (range: 16–56%) of the chemical compositions remain undisclosed due to commercial confidentiality. Notably, the undisclosed ingredients are predominantly employed in the photolithography process. The complex chemical condition involved in these semiconductor processes include strong acids, alkalis, and potent oxidants, and UV light is used in the photolithography process. Among the intricate blends of industrial chemicals in wastewater, various reactions may take place, including hydration, oxidation, sulfonation, amide formation, and nitration.

Additionally, during the biological treatment in wastewater treatment plants, reactions such as oxidation, deamination, desulfonation, and dicarboxylation occur [10, 37]. Due to the exceptional stability of the fluoroalkyl chain, reactions in the polar functional section led to distinct mass defect values for each transformation. This renders the use of homologous patterns for screening impractical. Our fragment-based approach overcomes the limitations of conventional homologous series. In total, we have identified 83 PFAS from 43 subclasses, with 29 substances reported for the first time. (Table 2).

Oxidation of FBSEE diol yields FBSEE diacid, while FBSE oxidation produces tentatively identified FBSAA, both with tentative identifications at CL 2b due to the

lack of standards [10]. A key distinction in current study is the inclusion of a standard for FBSAA confirmation. Through RT alignment and consistent MS2 spectra, (Fig. S14a) we verified the presence of FBSAA at 15.5 min with CL1a. Notably, an isomer of FBSAA with higher polarity presented at RT 9.9 min, showcasing distinct MS2 spectra (Fig. S14c) that suggest structural differences. Considering the potential isomerization between acid and diol forms [40], fragment analysis led to the proposal of a diol structure for the isomer (Fig. S14c). In addition, we introduce intermediate products of FBSE oxidation: FBSAcAL (RT 30.0 min, Fig. S18b) and its hydrated form as FBSAcAL hydrate (RT 30.0–32.6 min, Fig. S19), detected for the first time via mass spectrometry. Another structural isomer of FBSAcAL (7a-1) at RT 13.0 min was identified with higher polarity as its MS2 spectrum shown in Fig. S18a. Here, we propose an oxidation pathway, including the first publication of intermediate transformations of aldehyde (enol and keto form), aldehyde hydrate, and two isomers of FBSAA in Fig. 3.

### 3.4 Structural isomers from headgroup

FBSA-PrNO<sub>2</sub> and FBSE-Am are isomers with distinct polar head groups—sulfonamide and sulfonamido ethanol, respectively (Fig. 2). FBSA-PrNO<sub>2</sub> exhibit [SO<sub>2</sub>N]<sup>-</sup> fragment along with an additional signal for the neutral loss of C<sub>3</sub>H<sub>5</sub>NO<sub>2</sub>, categorizing it as miscellaneous FASAs (Subclass 1 h). In contrast, FBSE-Am demonstrates a specific signal at 121.9917, confirming its classification as FASEs, and its neutral loss of CONH categorizes it within the miscellaneous FASEs (Subclass 2 h). The RT of FBSA-PrNO<sub>2</sub> was 8.8 min, while that of FBSE-Am was 29.9 min, indicating significant differences in polarity. Thus, the headgroup isomers exhibit unique reactivity and physicochemical properties, may impact the variations in sludge metabolism during wastewater treatment in WWTPs [38]. Furthermore, E-FBSEs and FBSAcAL hydrate (Subclass 8a) are differentiated by their respective polar head groups: sulfonamido ethanol and sulfonamido acetaldehyde hydrate (Fig. 4). Specifically, fragment 121.9917 is

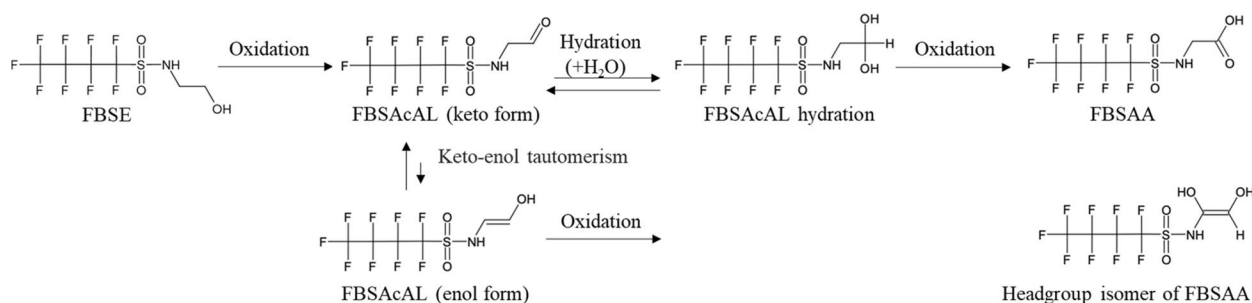


**Fig. 3** The oxidation pathway of FBSE to FBSAA involves intermediate compounds, including aldehyde and aldehyde hydration. Two isomers of FBSAcAL (keto and enol form) and two isomers of FBSAA were detected

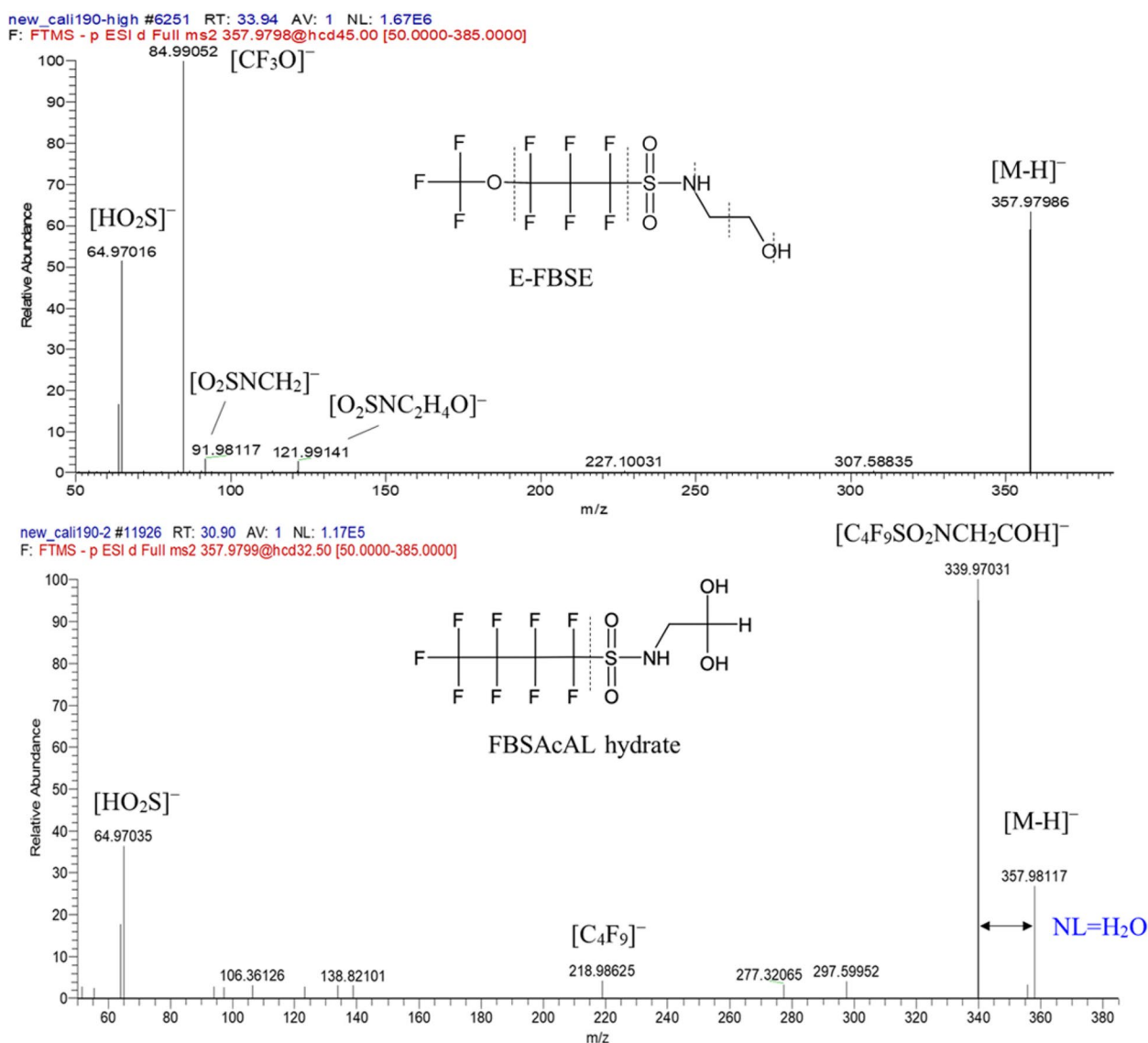


**Fig. 4** MS2 spectra of E-FBSE and FBSAcAL hydrate as polar head isomers

unique to sulfonamido ethanol, while the hydrate can be identified by the neutral loss of H<sub>2</sub>O. Finally, MeFBSAA and FBSPrA, which are polar head isomers, exhibit differences in the number of carbons in the sulfonamido carboxylic acid (Fig. S24). This clearly results in distinct neutral losses—one for acetic acid (CH<sub>2</sub>CO<sub>2</sub>) and the other for propanoic acid (C<sub>2</sub>H<sub>4</sub>CO<sub>2</sub>). Additionally, MeFASAA showed no [SO<sub>2</sub>N]<sup>-</sup> fragment signal, indicating solely the presence of only the [SO<sub>2</sub>F]<sup>-</sup> fragment signal due to N-methyl substitution. Conversely, FBSPrA exhibited a distinct [SO<sub>2</sub>N]<sup>-</sup> fragment, signifying the lack of additional N-substitution. The specific fragmentation patterns have been classified in Table 1. This investigation unveiled 25 isomeric PFAS, including isomers with different headgroups and functional tail groups.

These results emphasize the significance of understanding varied reactions and the overall composition of PFAS emissions in semiconductor wastewater, highlighting its complexity and posing challenges for subsequent wastewater treatment.

#### 4 Conclusions

For the nontarget PFAS approach, mass defect and homologous patterns are potent tools for uncovering PFAS within a series of homologous substances. However, industrial chemicals exhibit diverse and unique functional groups, making homologues less likely to occur in industrial manufacturing. Moreover, the intricate blend of industrial chemicals in wastewater may undergo diverse reactions, such as hydrolysis, oxidation

and deamination. As these reactions unfold in the polar functional section, each transformation leads to distinct mass defect values, rendering the use of homologous patterns for screening. Consequently, our research employs a fragment-based approach to investigate nontarget PFAS, particularly focusing on hydrophilic head groups, overcoming the limitations of conventional homologous series. Utilizing this approach, we successfully identified 83 PFAS in wastewater and effluent samples from semiconductor plants, including 29 newly discovered compounds, which are categorized into three groups (1) The presence of FBSE derivatives, FBSA derivatives, and FBSEE diol derivatives in the authentic standard implies that these derivative series detected in wastewater may stem from chemical formulation byproducts. They constitute less than 0.1–0.5% of the total area compared to main components like FBSE, FBSA, and FBSEE diol. These newly identified byproducts, displaying variations in fluoroalkyl chains such as hydrogen-substituted, unsaturated, and ether structures, were first identified in authentic standards, indicating their origin as byproducts of the chemical manufacturing process. (2) Compounds that undergo intermediate transformation compounds during the oxidation of FBSE, specifically perfluorobutane sulfonamido acetaldehyde and its hydrate, are newly identified. (3) Diverse reaction products generated from the intricate processes of semiconductor manufacturing, which utilize strong acids, bases, and solvents under UV light or heat conditions, include novel PFAS-related reaction compounds generated through hydrolysis, sulfonation and nitrification. We found that FBSA and FBSE reacted with chemicals used in the procedures of semiconductor, and the hydrogen of FBSA on N reacted with sulfonic acid, leading to the detection of several neutral losses during neutral loss screening. This underscores the significance of understanding PFAS-related reactions in semiconductor manufacturing.

In brief, these discoveries underscore the efficacy of the fragment-based approach in identifying unique industrial chemicals and its value in understanding diverse reactions and the actual emission compositions of PFAS in semiconductor wastewater. Moreover, under the Stockholm Convention's regulation for PFAS precursor elimination, complexity arises due to the absence of standards and standardized identification methods for diverse PFAS precursors, which undergo degradation to form terminal PFAS through the amendment of polar functional groups. This poses challenges in recognizing and quantifying the levels of products, complicating market surveillance. Our streamlined fragment-based approach addresses these hurdles and provides a strategic concept for identifying PFAS precursors, particularly those exhibiting versatility in polar functional groups.

## Supplementary Information

The online version contains supplementary material available at <https://doi.org/10.1186/s42834-024-00221-1>.

Supplementary Material 1.

### Acknowledgements

We extend our gratitude to Tzu-Hui Wang for her support in the pretreatment procedures and Meng-Chi Huang for his assistance in verifying the chemical structures.

### Authors' contributions

Yi-Ju Chen: study design, experimental work, data analysis, writing and editing manuscript. Jheng-Sian Yang: experimental work and editing manuscript. Angela Yu-Chen Lin: supervision and funding acquisition. The authors read and approved the final manuscript.

### Funding

Financial support for this study was provided by the Taiwan National Science and Technology Council through the following projects: MOST 111–2221-E-002–047-MY3 and MOST 111–2221-E-002–042-MY3.

### Availability of data and materials

All data generated or analyzed during this study are included within the article.

### Declarations

### Competing interests

The authors declare that they have no competing interest.

### Author details

<sup>1</sup>Ministry of Environment, National Environmental Research Academy, Taoyuan 320680, Taiwan. <sup>2</sup>Graduate Institute of Environmental Engineering, National Taiwan University, Taipei 106319, Taiwan.

Received: 6 February 2024 Accepted: 2 July 2024

Published online: 15 July 2024

### References

1. Gluge J, Scheringer M, Cousins IT, DeWitt JC, Goldenman G, Herzke D, et al. An overview of the uses of per- and polyfluoroalkyl substances (PFAS). *Environ Sci-Proc Imp.* 2020;22:2345–73.
2. Han J, Kiss L, Mei H, Remete AM, Ponikvar-Svet M, Sedgwick DM, et al. Chemical aspects of human and environmental overload with fluorine. *Chem Rev.* 2021;121:4678–742.
3. OECD. Reconciling Terminology of the Universe of Per-and Polyfluoroalkyl Substances: Recommendations and Practical Guidance, OECD Series on Risk Management, No. 61. Paris: Organisation for Economic Cooperation and Development; 2021.
4. Wang Z, Buser AM, Cousins IT, Demattio S, Drost W, Johansson O, et al. A new OECD definition for per- and polyfluoroalkyl substances. *Environ Sci Technol.* 2021;55:15575–8.
5. Olsen GW, Mair DC, Lange CC, Harrington LM, Church TR, Goldberg CL, et al. Per- and polyfluoroalkyl substances (PFAS) in American Red Cross adult blood donors, 2000–2015. *Environ Res.* 2017;157:87–95.
6. SIA. PFAS-Containing Surfactants Used in Semiconductor Manufacturing. Washington, DC: Semiconductor Industry Association; 2023.
7. SIA. PFAS-Containing Wet Chemistries Used in Semiconductor Manufacturing. Washington, DC: Semiconductor Industry Association; 2023.
8. SIA. PFOS and PFOA Conversion to Short-Chain PFAS-Containing Materials Used in Semiconductor Manufacturing. Washington, DC: Semiconductor Industry Association; 2023.
9. Lin AYC, Panchangam SC, Lo CC. The impact of semiconductor, electronics and optoelectronic industries on downstream perfluorinated chemical contamination in Taiwanese rivers. *Environ Pollut.* 2009;157:1365–72.

10. Chen YJ, Wang RD, Shih YL, Chin HY, Lin AY. Emerging perfluorobutane sulfonamido derivatives as a new trend of surfactants used in the semiconductor industry. *Environ Sci Technol.* 2024;58:1648–58.
11. Jacob P, Barzen-Hanson KA, Helbling DE. Target and nontarget analysis of per- and polyfluoroalkyl substances in wastewater from electronics fabrication facilities. *Environ Sci Technol.* 2021;55:2346–56.
12. Jacob P, Helbling DE. Rapid and simultaneous quantification of short- and ultrashort-chain perfluoroalkyl substances in water and wastewater. *ACS EST Water.* 2023;3:118–28.
13. Ojo AF, Peng C, Ng JC. Assessing the human health risks of per- and polyfluoroalkyl substances: A need for greater focus on their interactions as mixtures. *J Hazard Mater.* 2021;407:124863.
14. Evich MG, Davis MJB, McCord JP, Acrey B, Awkerman JA, Knappe DRU, et al. Per- and polyfluoroalkyl substances in the environment. *Science.* 2022;375:eabg9065.
15. USEPA. TSCA Section 8(a)(7) Reporting and Recordkeeping Requirements for Perfluoroalkyl and Polyfluoroalkyl Substances. Washington, DC: United States Environmental Protection Agency; 2024.
16. NEA. Potential PFBS and PFHxS Precursors – Literature Study and Theoretical Assessment of Abiotic Degradation Pathways Leading to PFBS and PFHxS. Trondheim: Norwegian Environment Agency; 2017.
17. Ateia M, Chiang D, Cashman M, Acheson C. Total oxidizable precursor (TOP) assay—best practices, capabilities and limitations for pfas site investigation and remediation. *Environ Sci Tech Let.* 2023;10:292–301.
18. Cioni L, Plassmann M, Benskin JP, Coelho ACMF, Nost TH, Rylander C, et al. Fluorine mass balance, including total fluorine, extractable organic fluorine, oxidizable precursors, and target per- and polyfluoroalkyl substances, in pooled human serum from the Tromsø population in 1986, 2007, and 2015. *Environ Sci Technol.* 2023;57:14849–60.
19. POPRC. Report of the Persistent Organic Pollutants Review Committee on the Work of its Fifteenth Meeting: Risk Management Evaluation on Perfluorohexane Sulfonic Acid (PFHxS), its Salts and PFHxS Related Compounds. In: Fifteenth meeting of the Persistent Organic Pollutants Review Committee (POPRC.15). Rome; 2019 Oct 1–4.
20. Zhao M, Yao Y, Dong X, Baqar M, Fang B, Chen H, et al. Nontarget identification of novel per- and polyfluoroalkyl substances (PFAS) in soils from an oil refinery in Southwestern China: a combined approach with TOP assay. *Environ Sci Technol.* 2023;57:20194–205.
21. Hensema TJ, Berendsen BJA, van Leeuwen SPJ. Non-targeted identification of per- and polyfluoroalkyl substances at trace level in surface water using fragment ion flagging. *Chemosphere.* 2021;265:128599.
22. Wang Y, Yu N, Zhu X, Guo H, Jiang J, Wang X, et al. Suspect and nontarget screening of per- and polyfluoroalkyl substances in wastewater from a fluorochemical manufacturing park. *Environ Sci Technol.* 2018;52:11007–16.
23. Wang X, Yu N, Qian Y, Shi W, Zhang X, Geng J, et al. Non-target and suspect screening of per- and polyfluoroalkyl substances in Chinese municipal wastewater treatment plants. *Water Res.* 2020;183:115989.
24. Zhang W, Pang S, Lin Z, Mishra S, Bhatt P, Chen S. Biotransformation of perfluoroalkyl acid precursors from various environmental systems: advances and perspectives. *Environ Pollut.* 2021;272:115908.
25. Zhang L, Lee LS, Niu J, Liu J. Kinetic analysis of aerobic biotransformation pathways of a perfluorooctane sulfonate (PFOS) precursor in distinctly different soils. *Environ Pollut.* 2017;229:159–67.
26. Charbonnet JA, McDonough CA, Xiao F, Schwichtenberg T, Cao D, Kaserzon S, et al. Communicating confidence of per- and polyfluoroalkyl substance identification via high-resolution mass spectrometry. *Environ Sci Tech Let.* 2022;9:473–81.
27. Fang B, Zhang Y, Chen H, Qiao B, Yu H, Zhao M, et al. Stability and biotransformation of 6:2 fluorotelomer sulfonic acid, sulfonamide amine oxide, and sulfonamide alkylbetaine in aerobic sludge. *Environ Sci Technol.* 2024;58:2446–57.
28. Mullin L, Katz D, Riddell N, Plumb R, Burgess JA, Jogsten IE. Reduction of LC/MS In-Source Fragmentation of HFPO-DA (GenX) Through Mobile Phase Additive Selection: Experiments to Increase [M-H]<sup>-</sup> Formation. In: DioXin 2018: 38th International Symposium on Halogenated Persistent Organic Pollutants, Krakow; 2018 Aug 26–31.
29. Zweigle J, Bugsel B, Zwiener C. FindPFAS: Non-target screening for PFAS—comprehensive data mining for MS<sup>2</sup> fragment mass differences. *Anal Chem.* 2022;94:10788–96.
30. Buck RC, Franklin J, Berger U, Conder JM, Cousins IT, de Voogt P, et al. Perfluoroalkyl and polyfluoroalkyl substances in the environment: terminology, classification, and origins. *Integr Environ Assess Manag.* 2011;7:513–41.
31. Paul AG, Jones KC, Sweetman AJ. A first global production, emission, and environmental inventory for perfluorooctane sulfonate. *Environ Sci Technol.* 2009;43:386–92.
32. Kissa E. *Fluorinated Surfactants and Repellents*. 2nd ed. Boca Raton: CRC Press; 2001.
33. Benskin JP, De Silva AO, Martin JW. Isomer profiling of perfluorinated substances as a tool for source tracking: a review of early findings and future applications. *Reviews of environmental contamination and toxicology.* 2010;208:111–60.
34. Loewen M, Halldorson T, Wang F, Tomy G. Fluorotelomer carboxylic acids and PFOS in rainwater from an urban center in Canada. *Environ Sci Technol.* 2005;39:2944–51.
35. Jin B, Liu H, Che S, Gao J, Yu Y, Liu J, et al. Substantial defluorination of polychlorofluorocarboxylic acids triggered by anaerobic microbial hydrolytic dechlorination. *Nat Water.* 2023;1:451–61.
36. Yang JS, Lai WWP, Lin AYC. New insight into PFOS transformation pathways and the associated competitive inhibition with other perfluoroalkyl acids via photoelectrochemical processes using GOTiO<sub>2</sub> film photoelectrodes. *Water Res.* 2021;207:117805.
37. Jin B, Zhu Y, Zhao W, Liu Z, Che S, Chen K, et al. Aerobic biotransformation and defluorination of fluoroalkylether substances (ether PFAS): substrate specificity, pathways, and applications. *Environ Sci Tech Let.* 2023;10:755–61.
38. Londhe K, Lee CS, McDonough CA, Venkatesan AK. The need for testing isomer profiles of perfluoroalkyl substances to evaluate treatment processes. *Environ Sci Technol.* 2022;56:15207–19.
39. Yoon C, Kim S, Park D, Choi Y, Jo J, Lee K. Chemical use and associated health concerns in the semiconductor manufacturing industry. *Saf Health Work.* 2020;11:500–8.
40. Rogers CO, Lockwood KS, Nguyen QLD, Labbe NJ. Diol isomer revealed as a source of methyl ketene from propionic acid unimolecular decomposition. *Int J Chem Kinet.* 2021;53:1272–84.

## Publisher's Note

Springer Nature remains neutral with regard to jurisdictional claims in published maps and institutional affiliations.